

## Adaptive Airfoil Wing for Micro UAV Flight Control

Martinez M.<sup>1</sup>, Chen Y.<sup>1</sup>, Wickramasinghe V.<sup>1</sup>, Wong F.<sup>2</sup>, Kraemer K.<sup>3</sup>

<sup>1</sup>National Research Council Canada, Institute for Aerospace Research  
Structures & Materials Performance Laboratory  
1200 Montreal Road, Ottawa, Ontario, K1A 0R6, Canada  
Email: marcias.martinez@nrc-cnrc.gc.ca  
Phone: (613) 991-5360

<sup>2</sup>Defence Research & Development Canada - Valcartier  
2459 Pie-XI Blvd North, Québec, Quebec, G3J 1X5 Canada.  
Email: Franklin.Wong@drdc-rddc.gc.ca  
Phone: (418) 844-4000 ext. 4200

<sup>3</sup>Directorate of Technical Airworthiness and Engineering Support  
Department of National Defence Canada

### ABSTRACT

Design of an adaptive airfoil wing for Micro Unmanned Air Vehicle flight control is being considered. The smart wing structure would consist of a composite spar supporting several Macro Fiber Composite actuators under a preload condition. The preload would be exerted on the actuators by an Electro Active Polymer skin. The active skin is being considered to augment the actuation performance of the wing. A deflection angle of 30° to 40° is proposed as the requirement for the design concept. A Finite Element Analysis has been performed to verify the deflection of the adaptive wing in wind-off conditions. Shape change is accomplished by the control of integrated Lead Zirconate Titanate (PZT) based Macro Fiber Composite (MFC) elements. An actuation design study is performed from an analytical characterization model and verified using the Finite Element Method (FEM). The analytical model assumes that deformation of the structure occurs due to the applied electric potential on the electro active polymer skin and the MFC actuators. Wind-on surface pressure conditions are calculated using XFOIL and applied in a loosely-coupled fluid-structure analysis to estimate wing deflections.

*Key Words: Adaptive airfoil Wing, AFC, MFC, PZT, Actuated Fiber Composites, Piezoelectric Fibers.*

### 1. INTRODUCTION

Researchers and Engineers are making use of smart structures for small and large scale applications. As technology advances there is a need for “biological-like” materials that are more efficient and capable in sensing and actuating. Piezoelectric materials can provide such functions; however, if piezoelectric materials are to be more widely used in engineering applications, they will be mostly in the form of composites. Bulk piezoelectric materials have several serious drawbacks impeding their use in many applications. The brittle nature of piezoelectric materials limits their widespread implementation. Most piezoelectric materials are ceramics with inherently low toughness that limits their use in any critical application. A number of brittle materials have been used for structural applications in the form of

fibers in fiber reinforced composite materials. Such composites provide materials with high strength and high toughness. Recently, several attempts were made to develop composite materials with piezoelectric fibers, while some are commercially available [1,2,3,4,5]. Such Active Fiber Composites (AFC) and Macro Fiber Composites (MFC) can be used as actuators and/or sensors in a number of different applications such as structural health monitoring (SHM) [6, 7] and integral structural actuators [8, 9]. It is the objective of this paper to analyze the linear and non-linear behavior of piezoelectric active composites for the development of an adaptive airfoil wing for a Micro UAV.

The use of smart structures has been investigated for a variety of aerospace applications including micro UAVs. Recently several helicopter manufacturers and researchers have analyzed and implemented the use of piezoelectric actuators for the development of active trailing edge flaps [10,11]. Several researchers have published papers on the use of MFC for active control of morphing of wings. It was shown in [12] that the use of MFC as a typical piezoelectric bending actuator (PBA) can produce large deformation at the trailing edge (over 16° peak to peak). The author also was able to show that the application of a preload on the PBA by means of a skin has a positive effect in achieving these high deformations.

Apart from the MFC composite actuator, another type of material that has been considered for smart materials structures is dielectric Electro Active Polymer (EAP). Dielectric EAP is a special type of polymer that has the ability to generate large deformation under an electric field. Usually, the EAP material is sandwiched between two very compliant electrodes in the form of a capacitor. Under a high electric field, the EAP material stretches due to the Maxwell's stress and the deformation is quadratic in nature. Therefore, the EAP material itself is not electro-active, but passive in nature [13, 14]. EAPs have been modeled by other researchers in order to understand their behavior and performance characteristics by using proprietary FEA packages [15]. Typical dielectric type EAP materials are commercially available from 3M<sup>TM</sup> (VHB4910).

This paper presents a unique active wing concept for micro UAV flight control applications. The design involves an active wing model based on the combination of MFCs as the primary bending control actuators and thin layers of EAP materials as the secondary active skin actuator to enhance the actuation capability. Integration of the two actuation mechanisms can generate a unique synergetic enhancement to the airfoil trailing edge deflection, which results from the reverse piezoelectric effect of the piezoelectric bimorph ribs, buckling effect on the rib from the compressive axial load of the pre-strained skin and electrostatic effect of the dielectric EAP skin. This innovative active airfoil concept is expected to generate significantly higher deformation for effective UAV flight control, but remains compact and light in weight, which is beyond other similar concepts.

## **2. Active Wing Model**

The active wing model consists of a NACA 0009 profile with active piezoelectric fiber actuators forming the active trailing edge as shown in Figure 1. The upper and lower skins of the wing are in tension thus increasing the actuation deflection of the aileron as identified in [12]. The skin is interconnected to tension rollers that will permit varying the tension load during the initial experimental investigation. The center spar is designed to join the active trailing edge with the composite leading edge. Both the leading edge and the active aileron is designed to be detached easily from the composite spar. The overall dimension of the trailing edge is 100 mm while the composite spar is 5.91 inches for an overall chord of 9.375 inches. The span of the prototype active wing section is approximately 9.375 inches.

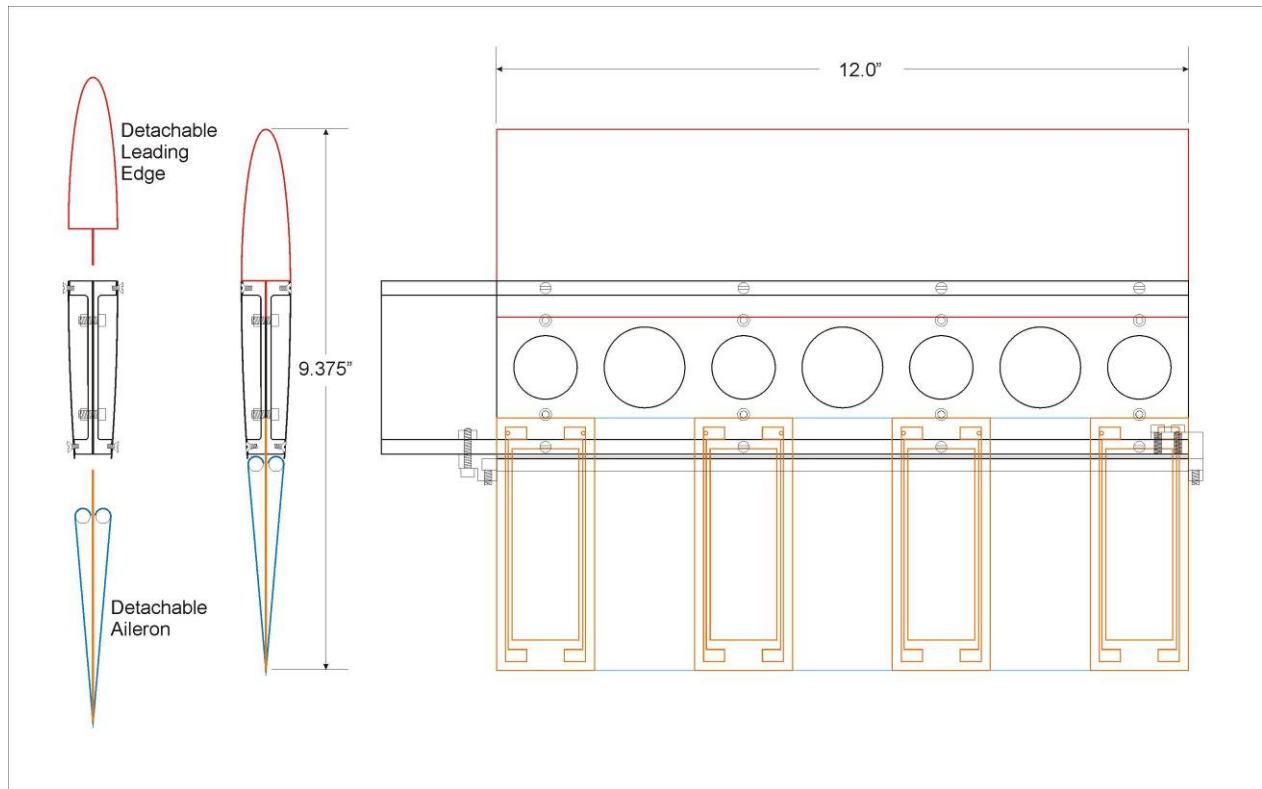


**Figure 1: Active Trailing Edge Wing**

This active trailing edge wing makes use of an active skin concept where the skin provides a preload on the MFC structure and aids in the actuation of the structure thus increasing the deformation of the active structure. The skin, made out of EAP material (3M<sup>TM</sup> - VHB4910), would be covered by a very compliant electrode required in the actuation of the active skin.

The center spar section of the wing is fabricated from carbon fiber pre-preg and acts as a clamp between the trailing edge and the leading edge of the wing. The leading edge is fabricated out of an inner foam core covered by woven carbon fiber pre-preg in order to provide the required smoothness and rigidity.

### 2.1. Piezoelectric Analytical Model and Results

Many researchers have studied piezoelectric cantilever beam actuators to predict the deflection under external control voltages. For example, Park [16] developed the bending and torsion models of a cantilever beam under piezoelectric induced-strain. Smits [17] and Devoe [18] studied the constituent equations of piezoelectric bimorph micro-actuators. Weinberg [19] further extended the equations to accommodate multiple layers of micro-piezoelectric MEMS actuators. In this section, equations are developed to predict the deflection of a MAV flap actuator equipped with two layers of piezoelectric actuators. The influence of multi external loads, including the axial pretension force, out-of-phase force and distributed aerodynamic load are considered to predict the natural frequency and deflection of the MAV aileron actuator for flight control applications. It is important to note that the model described here does not couple the piezoelectric and mechanical effects. In this model these are accounted for independently and then superimposed.

As shown in Figure 2, the MAV flap actuator is configured as a cantilever beam. Two layers of piezoelectric actuators are bonded to the top and bottom of a substrate plate symmetrically. Out-of-phase control voltages are applied to the two piezoelectric actuators to generate bending actuation authority. The substrate, bonding layer and the piezoelectric actuators are designed with the same width, but different thickness.

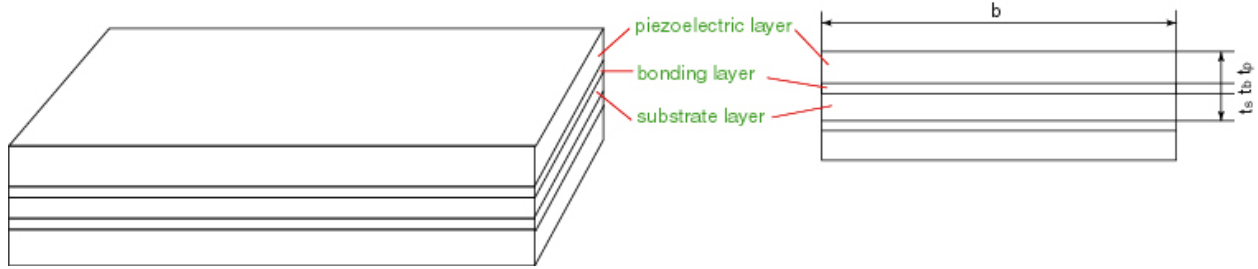


**Figure 2: MAV flap actuator configuration**

The model assumes that the bonding and substrate layers are isotropic and purely elastic. The interfaces between each layer are continuous and without slip. The piezoelectric layer is polarized in the thickness direction ( $d_{31}$ ). When voltage is applied, in-plane deformation will be generated. It also assumes that the thickness of each layer is small compared to the radius of deflection curvature induced by external loads. Since the width of the cantilever beam is generally much larger than the thickness, the beam can be considered as an in-plane strain situation. Therefore, the Young's Modulus  $E$  and piezoelectric strain coefficients ( $d_{31}$ ) used below can be replaced by:

$$E = E / (1 - \nu^2) \quad (1)$$

$$d_{31} = d_{31} (1 + \nu) \quad (2)$$

Where,  $\nu$ , is the poisson's ratio. The equilibrium equation of the MAV flap beam actuator is expressed as:

$$\frac{d^2 z}{dx^2} = \frac{M_\Lambda}{EI} + \frac{P_A z}{EI} + \frac{F_Z(L-x)}{EI} + \frac{\int_0^L p_x b(L-x) dx}{EI} \quad (3)$$

Where  $M_\Lambda$  represents the bending moment introduced by the two piezoelectric actuators;  $P_A$  is the axial preload;  $F_Z$  is the lumped out-of-phase force and  $p_x$  is the distributed pressure along the surface of the cantilever beam. The thickness and width of each layer in the cantilever beam are shown in Figure 2. Under the assumption of a uniform strain distribution within the cross-section of the piezoelectric actuators, the introduced piezoelectric control moment,  $M_\Lambda$ , can be described as [1]:

$$M_\Lambda = -E_p b_p \Lambda (t_p^2 + t_b t_p + 2t_s t_p) \quad (4)$$

Where,  $\Lambda$  is the free strain of the piezoelectric actuators under external control voltage (V) for a piezoelectric patch actuator polarized in the thickness direction ( $t_p$ ).  $\Lambda$  can be described as:

$$\Lambda = d_{31} \frac{V}{t_p} \quad (5)$$

The bending stiffness of the multilayer cantilever beam,  $EI$ , can be described as:

$$EI = \frac{1}{12} E_b b_b t_b^3 + 2E_p b_p t_p \left( \frac{1}{12} t_c^2 + \left( \frac{t_b}{2} + \frac{t_p}{2} + t_s \right)^2 \right) + 2E_s b_s t_s \left( \frac{1}{12} t_s^2 + \left( \frac{t_b}{2} + \frac{t_s}{2} \right)^2 \right) \quad (6)$$

In the case of Micro Fiber Composite (MFC) actuators where the piezoelectric strain coefficient  $d_{33}$  is used to replace the piezoelectric patches, the free strain should be replaced by:

$$\Lambda = d_{33} \frac{V}{t_{electrode}} \quad (7)$$

Where  $d_{33}$  represents the equivalent piezoelectric strain coefficient of the MFC;  $t_{electrode}$  is the distance between the interdigitated electrodes.

From equation 3, it is important to note there exists a nonlinear coupling between axial preload  $P_A$  and the cantilever beam deflection. By properly applying a compressive axial preload, the deflection of the MAV aileron actuator can be effectively improved without increasing the control voltage on the piezoelectric actuators. However, the natural frequency of the MAV flap actuator will also be shifted accordingly, as expressed in equation 8:

$$\omega_n^2 = \left( \frac{n\pi}{l} \right)^4 \left[ \frac{EI}{\rho A} \left( 1 - \frac{F_a L^2}{n^2 \pi^2 EI} \right) \right] \quad (8)$$

For the first natural frequency,  $n\pi = 1.875$ . Since a pre-compressive axial load will effectively reduce the natural frequency of the MFC flap actuator, the critical preload will be determined by

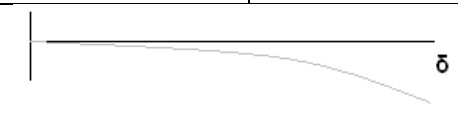
$$F_{cr} = \frac{3.52EI}{L^2} \quad (9)$$

Compared to PZT ceramic wafers that use the  $d_{31}$  coefficient, the MFC actuators use the higher  $d_{33}$  coefficient in order to generate larger deflections. MFC actuators are piezoceramic fibers embedded in a composite structure and they are able to survive larger external mechanical deformations. Therefore, MFC actuators are used in the development of an active wing concept for micro UAV applications. To estimate the performance of the active wing concept, preliminary analysis was conducted to predict the deformation under typical flight conditions. To facilitate the prediction, material and geometrical properties have been assigned to the MFC actuators, where Young's Modulus equals  $3.0 \cdot 10^{10}$  Pa; MFC thickness is 300 micrometers;  $d_{33}$  is  $400 \cdot 10^{-12}$  V/m with an interdigitated electrode spacing of 0.5 mm. The Aluminum substrate is assigned a Young's Modulus of  $7 \cdot 10^{10}$  Pa and a thickness of 76 micrometers. The bonding layer is assigned a Young's Modulus of  $3.378 \cdot 10^9$  Pa and a thickness of 31 micrometers. The overall dimensions of the actuator configuration are 35 mm by 95 mm. The activation voltage was set to 1500V.

The results obtained from the analytical study are shown in Table 1. The results indicate that the greater the compressive axial preload applied on the active wing, the greater the tip deflection is expected on the piezoelectric bending actuator. It is important to note that the limit of the axial compressive load is the buckling load of the bending actuator. It is noted that the axial compressive load on the piezoelectric actuator can be simultaneously achieved by properly pre-stretching the active EAP skin on the airfoil. Under an axial compressive preload of 20N,

1500V voltage on the MFC actuator and 5 layers of EAP skin, the combined deflection is predicted to be as high as 45.2mm.

**Table 1: Results from the Piezoelectric Analytical Model**

<b>MFC Actuator with Latex Skin &amp; Preload</b>				
	<b>Newtons</b>	<b>mm</b>	<b>mm</b>	<b>mm</b>
<b>Axial Load</b>	0	23.6		
<b>Axial Load</b>	10	29.7		
<b>Axial Load</b>	20	37.0		
<b>MFC Actuator with EAP Film and Preload</b>				
<b>EAP Film Layer</b>		1	3	5
<b>Axial Load</b>	0	24.7	26.7	28.8
<b>Axial Load</b>	10	31.0	33.6	36.3
<b>Axial Load</b>	20	38.7	41.9	45.2

## 2.2. Aerodynamic Model and Results

Aerodynamic loading constitutes one of the major factors that affect the performance of the smart wing actuation and the resultant deformation. The actuators and stiffness of the underlying structure must be able to maintain the desired aerodynamic shape to generate the control forces that manoeuvre the air vehicle. Methods exist to treat the coupled aero-elastic problem ranging from direct schemes [20] to fully coupled schemes [21] to sequential schemes [22]. As a first approximation to examine the fluid-structure interaction, aero-loads calculated in this section were applied to the smart wing structure in a single step before calculating the resultant structural deformations.

The aerodynamic loads were calculated according to the flight conditions shown in Table 2. The conditions cover the range of flight regimes that the smart wing is expected to see in a typical mission. Slow reconnaissance implies slow forward flight with the ability to make aggressive manoeuvres if required. Dash implies fast forward flight to transit between points of interest with only small course corrections. Cruise is an intermediate condition between ‘slow recon’ and ‘dash’. Positive flap deflection was defined in the direction of positive  $y$ .

To facilitate the analysis, the smart wing airfoil was approximated by the NACA 0009 geometry (Figure 3). The hinge line for the control surface was located at the normalized chord coordinate  $x/c = 0.6$  where  $x$  is the distance measured from the leading edge and  $c$  is the chord length. The normalized thickness at the hinge line was  $y/c = 0.0684$  where  $y$  is the total thickness. The maximum airfoil thickness was located at  $x/c = 0.3$ .

**Table 2 Flight Conditions**

<b>Operation</b>	<b>Speed (m/s)</b>	<b>Angle of Attack (deg)</b>	<b>Flap Deflection (deg)</b>
slow recon	2.8	-5 to +8	± 20
cruise	8.3	-3 to +3	± 10
dash	13.9	-2 to +2	± 5

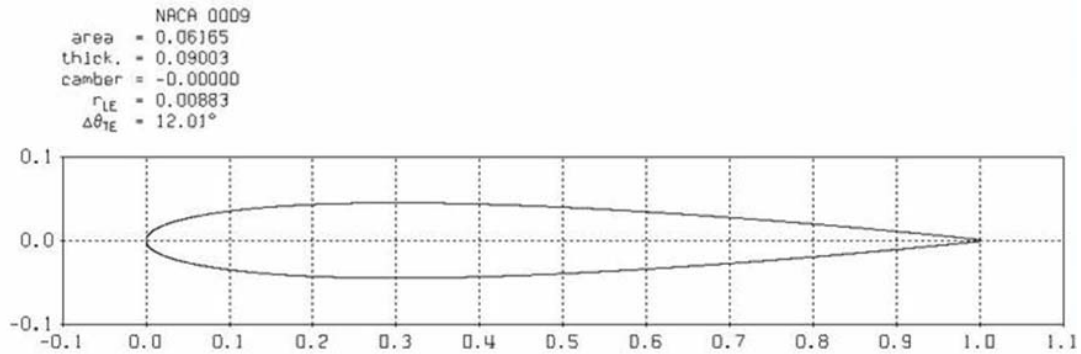


**Figure 3: Idealized Smart Wing airfoil using the NACA 0009 geometry**

The Xfoil program by Drela [23] was used to calculate the surface pressures on the airfoil with deflected surfaces. The code is capable of inviscid and viscous analysis of existing airfoils and allows predictions just beyond stall. The inviscid option was used to calculate the pressure coefficient results for -5, 0, +5° angle of attack with 0° flap deflection. The viscous option was used to generate the results for flap deflections of +2, +5, and +20° at 0° angle of attack. A typical set of results is shown graphically in Figure 4.

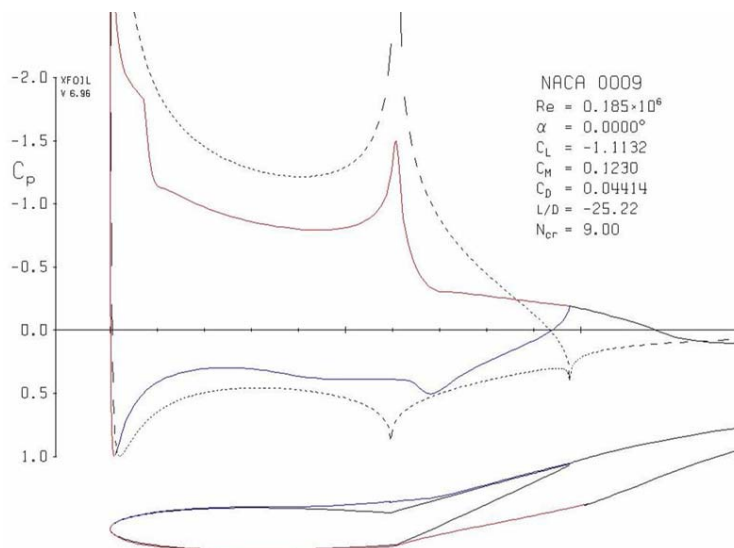


**Figure 4: Pressure coefficient results for a NACA 0009 geometry with a 20 deg. flap deflection at 'slow recon' speed.**

The viscous solutions were obtained by following the procedure outlined in the Xfoil User Primer [23]. The Reynolds number, based on a 250 mm characteristic chord length, was  $2.4 \cdot 10^5$  for 'dash' speeds while the 'cruise' and 'slow recon' were  $1.43 \cdot 10^5$  and  $0.48 \cdot 10^5$ , respectively. These values are in a flow regime where an accurate estimation of transition is needed for the calculation of representative surface pressure coefficients. Xfoil uses the  $e^n$  method for free transition [23]. The default  $N_{crit} = 9$  was used for the calculations.

The surface pressure in engineering units was calculated according to:

$$P = (1/2) C_p \rho V_{fs}^2 \quad (10)$$

Where,  $C_p$  is the local pressure coefficient,  $\rho$  is  $1.225 \text{ kg/m}^3$ , and  $V_{fs}$  is the free stream velocity.

Table 3, shows the results of the tip deflection of the active trailing edge with and without aerodynamic loading. As seen in Table 3, several pressure loads on the trailing edge section were considered (triangular vs. uniform pressure loading). The uniform pressure load assumes that the entire trailing edge has a constant pressure profile over the wing. The amplitude of the constant pressure load is equivalent to the pressure at the root of the trailing edge. The triangular pressure load assumes that the pressure load is not uniform but it has a linear reduction in pressure from the root of the trailing edge to the tip. As seen from the analytical model, the loss in deflection is not significant when comparing the effect of the different aerodynamic profiles on various axial pre-load conditions.

**Table 3: Tip deflection of the Active Trailing Edge with Aerodynamic loading (based on the analytical model)**

Axial preload (N)	Without Aerodynamic Load (mm)	With Aerodynamic Profile Load ( $\Delta P=300\text{Pa}$ )			
		MFC Beam Flap		MFC Beam Flap with Latex Skin	
		Triangular (mm)	Uniform (mm)	Triangular (mm)	Uniform (mm)
<b>0</b>	23.6	23.3	19.9	21.2	18.7
<b>1</b>	24.2	23.8	20.4	21.6	19.1
<b>5</b>	26.5	26.1	22.2	23.7	20.9
<b>10</b>	29.7	29.2	24.7	26.5	23.2

### 2.3. Piezoelectric FEM Model and Results

A FEA solver was developed in [2]. The FEA solver makes use of the PARDISO sparse solver available through the Intel Math Kernel Library (IMKL). The implementation of IMKL includes multi-core processing capabilities and was compiled in both 32 and 64 bit window operating system. The solver makes use of both 8 and 20 node brick elastic and piezoelectric elements. All simulations presented in this work were modeled in a Windows XP 64 bit Machine with 2 Intel Core 2 Extreme (CPU Q6850) and 8 Gb of RAM.

The trailing edge finite element (FE) model is shown in Figure 5. The aluminum substrate is sandwiched between two MFCs. Each MFC is bonded to the aluminum substrate with a very thin layer of adhesive. The MFCs were purchased from Smart Material Corporation [5] and modeled accordingly. The actual PZT fibers and electrode width and spacing were measured using an optical microscope (Nikon Eclipse L150). The measured parameters were utilized to develop the FE model in Figure 5. The leading edge of the wing was not modeled since it did not contain any active components.



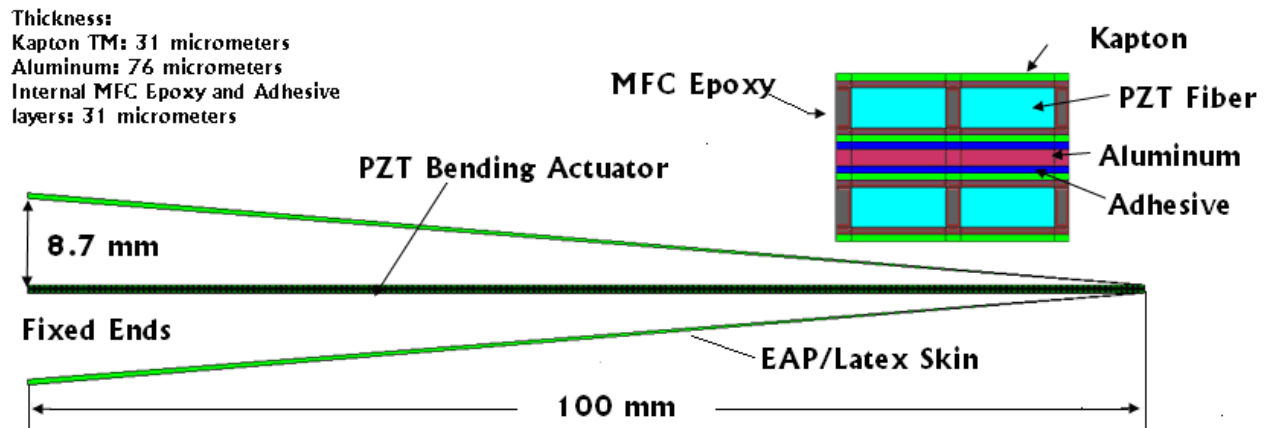


Figure 5: Trailing Edge FE Model

The models were constructed using the material properties for PZT-5A fibers, an epoxy matrix, four Kapton™ layers, two adhesive layers and an aluminum substrate. The piezoelectric fibres in the MFC model have the following piezoelectric parameters:  $d_{33}$  of  $374 \cdot 10^{-12}$  C/N,  $d_{31}$  of  $171 \cdot 10^{-12}$  C/N, and  $d_{24}$  and  $d_{15}$  of  $584 \cdot 10^{-12}$  C/N. Mechanical properties were modeled using the following constants:  $C_{11}=120$  GPa,  $C_{33}=110$  GPa,  $C_{44}=21$  GPa,  $C_{66}=23$  GPa,  $C_{12}=75.2$  GPa and  $C_{13}=75.1$  GPa [24]. The MFC epoxy and adhesive layers had a Young's modulus of 3.38GPa and Poisson's ratio of 0.33. The Kapton™ had a Young's modulus of 2.5 GPa and Poisson's ratio of 0.34. Finally, the aluminum was modeled with a Young's modulus of 70 GPa and a Poisson's ratio of 0.33.

The active skin was modeled using a Young's Modulus of  $3.1 \cdot 10^4$  Pa and a Poisson's ratio of 0.3. Both the latex and the electro active skin were assumed to have the same material properties. The FE solver does not solve non-linear problems, thus the FEA performed assumed linear deformation of the structure without pre-load and a latex skin.

The MFC structure was modeled such that the upper MFC extended while the lower MFC contracted, thus creating a piezoelectric bending actuator. The electric potential for each MFC was set independently as shown in Figure 6. The maximum electric potential was set to 1500 Volts as indicated by the MFC manufacturer [5].

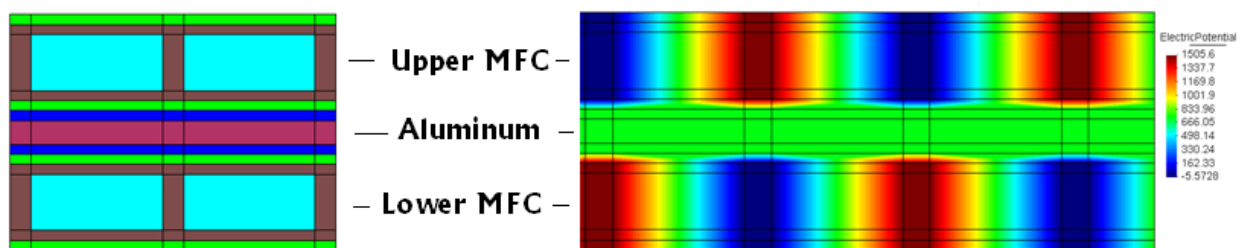


Figure 6: Electric Potential Configuration

The deformation of a 100mm trailing edge with a latex skin is shown in Figure 7. The FE model does not include an axial preload, aerodynamic loading and uses a linear elastic deformation with electro-mechanical coupling. The results indicate that the FE model and the analytical model agree very closely.

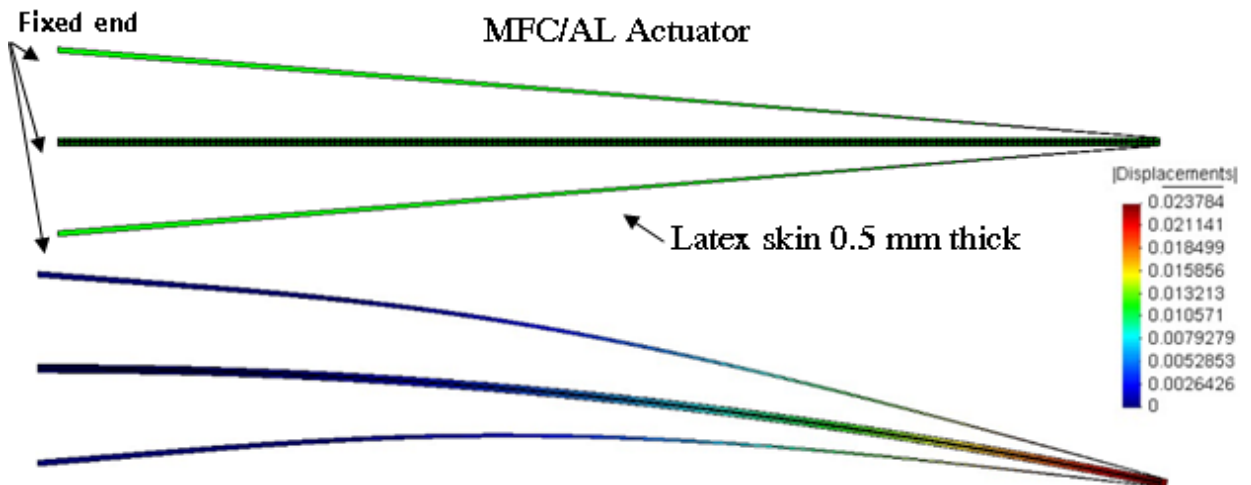


Figure 7: FE Model of an Active Trailing Edge Wing (Displacement in meters)

In the FE model, a variable aerodynamic loading was applied on the MFC structure assuming a triangular pressure distribution. The results indicated that the effect of aerodynamic loading on the PBA is negligible and that the maximum tip deflection reduces from 23.8 mm to 23.1 mm. It is also important to observe that if that same aerodynamic loading is applied directly on the skin this will most likely produce a large impact on the shape of the skin. The bottom skin could potentially collapse directly on the MFC structure while the upper skin would produce a bubble shape. This effect could not be analyzed in the FE model due to the non-linear nature of this problem. However, a pre-stretched latex skin will help to reduce the skin deformation due to aerodynamic load and mitigate the possible collapse or bubble shape effect.

When an aerodynamic pressure load of 300 Pa uniformly distributed over the trailing edge was simulated, the maximum tip deflection achieved (no axial load) was 16.8 mm vs. 18.7mm from the analytical model. The 2.1 mm difference is due to the fact that the analytical model assumes superposition while the FE model is based on solving the coupled electro-mechanical constitutive equations.

### 3. Conclusions

It has been shown that a combination of an active skin with a preload can produce larger tip deflection on a PBA. The results were demonstrated through both an analytical and piezoelectric linear elastic FE model. The results show that the effects of aerodynamic loading on the PBA are not significant but that they could produce a large deformation when applied to the active skin. It was demonstrated that the analytical model was accurate as long as the applied pressure loads are small. If the pressure loads increase the difference between the analytical and FE model will become greater. A non-linear FE model will be required to validate the effect of axial pre-loading on the PBA. A FE model will also be required to model the behavior of EAP skin.

*Acknowledgement* - This work was financially supported by Defence Research Development Canada and the National Research Council Canada.

### 4. References

- [1] M. Martinez, A. Artemev, F. Nitzsche, B. Geddes, Finite Element Modeling of Actuated Fibre Composites, Conference proceeding for HSPM 2006, Ostend-Belgium May 3-4, 2006.

**19<sup>th</sup> International Conference on  
Adaptive Structures and Technologies**

October 6-9, 2008  
Ascona, Switzerland

- [2] M. Martinez, M. Melnykowycz, A. Artemev, F. Nitzsche, Finite Element Analysis of Actuated Fiber Composites, Cansmart 2005, International Workshop, Smart Materials and Structures, 13 - 14 October 2005, Toronto, Ontario, Canada.
- [3] Internal Report: Prof. Dr. Paolo Ermanni, Benedetto Castelli, Alberto Belloli, Modeling and Characterization of Active Fiber Composites Diploma Thesis at the Centre of Structure Technologies, Institute of Mechanical Systems, Department of Mechanical and Process Engineering, ETH Zurich IMES Ref.-Nr: 08-183.
- [4] Cu-Hai Nguen and Xavier Kornmann, A Comparison of Dynamic Piezoactuation of Fiber-based Actuators and Conventional PZT Patches Journal of Intelligent Material Systems and Structures, Vol. 17—January 2006 pp.45.
- [5] <http://www.smart-material.com/>, Last accessed on: June 19, 2008
- [6] K.I. Salas and C.E.S. Cesnik, Design, Characterization and Modeling of the CLoVER Transducer for Structural Health Monitoring, Proceedings of the fourth European Workshop, Structural Health Monitoring 2008, Cracow Poland, pp. 441.
- [7] D.C. Zhang, P. Qing, T. Chang and I. Li, New Multifunctional Hardware Platforms for Comprehensive SHM, Proceedings of the fourth European Workshop, Structural Health Monitoring 2008, Cracow Poland, pp. 373.
- [8] Chopra, I., "Review of State of Art of Smart Structures and Integrated Systems," American Institute for Aeronautics and Astronautics Journal, Vol. 40, No. 11, 2002, pp. 2145-2187.
- [9] Bent, A. A., Hagood, N. W. and Rodgers, J. P. "Anisotropic Actuation with Piezoelectric Fiber Composites," Journal of Intelligent Material Systems and Structures, Vol. 6, 1995, pp.338-349.
- [10] Elif Ahchi, Rupert Pfaller, Structural Design, Optimization and Validation of the Integrated Active Trailing Edge for a Helicopter Rotor Blade, Proceeding of the 64<sup>th</sup> Annual Forum of the American Helicopter Society, Montreal, April 2008.
- [11] Smith Thepvongs, Carlos E.S. Cesnik, Finite-State Aeroelastic Modeling of Rotating Wings with Deformable Airfoils, Proceeding of the 64<sup>th</sup> Annual Forum of the American Helicopter Society, Montreal, April 2008.
- [12] Roelof Vos, Post-Buckled Precompressed Elements: A New Class of Control Actuators for Morphing Wings UAVs, Journal of Aircraft, Vol. 44, No. 4, July–August 2007
- [13] Guggi Kofod, Peter Sommer-Larssen, Roy Kornbluh and Ron Pelrine, Actuation Response of Polyacrylate Dielectric Elastomer, Journal of Intelligent Material Systems and Structures, Vol. 14, Dec. 2003
- [14] Peter Sommer-Larssen, Guggie Kofod, Shridhar MH, Mohammed Benslimane, Peter Gravesen, Performance of dielectric elastomer actuators and materials, Smart Structures and Materials, Proceeding of SPIE Vol. 4695, 2002.

**19<sup>th</sup> International Conference on  
Adaptive Structures and Technologies**

October 6-9, 2008  
Ascona, Switzerland

- [15] G. Yang, G. Yaho, W. Ren, G. Akhras, J.P. Szabo and B.K. Mukherjee, "The Strain response of silicone dielectric elastomer actuators", *Proceeding of the SPIE International Symposium on Smart Structures and Materials*, San Diego USA, 2005.
- [16] Park, C. , Walz, C. and Chopra, I., "Bending and Torsion Models of Beams with Induced-Strain Actuators ", *Smart Materials and Structures*, Vol. 5 (1996):98-113.
- [17] Smits, J. and Choi, W. S., "The Constituent Equations of Piezoelectric Heterogeneous Bimorph", *IEEE Transactions on Ultrasonics, Ferroelectrics and Frequency Control*, Vol. 38 (3), 1991."
- [18] Devoe, D. and Pisano, A., "Modeling and Optimal Design of Piezoelectric Cantilever Microactuators", *Journal of Microelectromechanical Systems*, Vol. 6, No. 3, 1997.
- [19] Weinberg, M. S., "Working Equations for Piezoelectric Actuators and Sensors", *Journal of MEMSW*, Vol.8, No. 4, 1999.
- [20] Bisplinghoff, R.L., Ashley, H., *Principles of Aeroelasticity*, Dover Publications Inc., New York (1962).
- [21] Spadoni, A., Ruzzene, M., "Static Aeroelastic Response of Chiral-core Airfoils", *J. Intell. Mater. Syst. and Struct.*, Vol. 18, pp. 1067-1075 (2007).
- [22] Farhat, C., Lesoinne, M., "Two efficient staggered algorithms for the serial and parallel solution of three-dimensional nonlinear transient aeroelastic problems", *Comp. Methods Appl. Mech. Engng.*, Vol. 182, pp. 499-515 (2000).
- [23] <http://web.mit.edu/drela/Public/web/xfoil/> Last accessed on July 29, 2008.
- [24] [http://www.efunda.com/materials/piezo/material\\_data/matdata\\_output.cfm?Material\\_ID=PZT-5A](http://www.efunda.com/materials/piezo/material_data/matdata_output.cfm?Material_ID=PZT-5A), Last accessed on June 19, 2008.